ARIEL VI MEASUREMENTS OF ULTRA-HEAVY COSMIC RAY FLUXES IN THE REGION Z $\geq$ 48

P.H. Fowler, M.R.W. Masheder, R.T. Moses,
R.N.F. Walker, A. Worley and A.M. Gay
H.H. Wills Physics Laboratory, University of Bristol,
Tyndall Avenue, Bristol BS8 1TL, England.

1. Introduction. The Bristol cosmic ray detector on the Ariel VI satellite is described briefly in OG4.4-3 and more fully in Ref.(1). The data for charges Z $\geq$ 48 discussed in this paper were obtained with the same data selection and analysis criteria set out in OG4.4-3, except that, for this high charge region, pollution from slowing iron nuclei is not possible and data collected at all vertical cut-offs may be used.

For this re-analysis of the Ariel VI data, the contribution of non-Z^2 effects to the restricted energy loss and to Cerenkov radiation in the Bristol sphere has been evaluated using the Mott cross section ratios tabulated in (2) and the non-relativistic Bloch correction given clearly in (3). Results obtained were similar in form to those derived for HEAO3 by Derrickson et al. (4) but with maximum deviations ~10% rather than 15% for the Mott term, corresponding to a thinner detector. Because of the large uncertainties in the parameters involved, no relativistic Bloch term was included; in any case Waddington et al.(5) found no significant deviation from Mott plus non-relativistic Bloch in their experimental work. In addition the experiments of Garrard et al. (6) on the HEAO detector make the application of a correction to the Cerenkov response of doubtful justification and none has been applied in this analysis. An energy dependent correction was made using an effective energy calculated from the vertical cut-off for a given event. The maximum value of this correction was about 0.6% in Z for low cut-offs, declining to ~ zero by 10 GV.

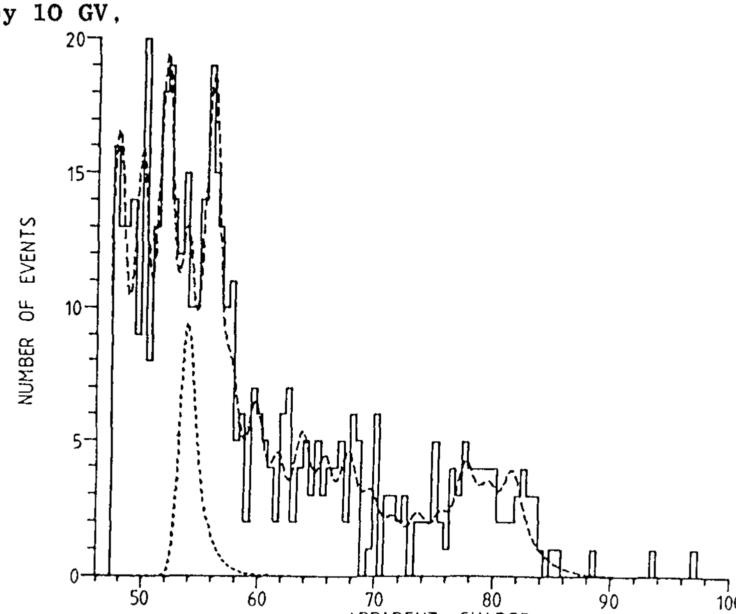

Fig. 1 Distribution of accepted data for determination of Z $\geq$ 48 abundances. Dotted insert shows distribution of $_{54}$Xe content (Table 1)

2. Results. Fig.1 shows the distribution of data for all charges $Z \geq 48$. These events were accompanied by 8.68×10^6 $_{26}Fe$ nuclei. In this distribution all events were collected at the highest priority and numbers given are actual numbers of detected events. The resolution function for $_{54}Xe$ is shown as a dotted insert and clearly resolved peaks are seen for $_{52}Te$ and $_{56}Ba$. A similar procedure of deconvolution was followed for this data to that described in OG4.4-3, but with a resolution function supplied only for each even charge, odd abundances being set to zero. The derived numbers are shown in column 2 of Table 1. The peaks at $_{52}Te$ and $_{56}Ba$ in Fig.1 are seen to be consistent with the predicted resolution, as is the precipitate fall from Z = 56 to Z = 60.

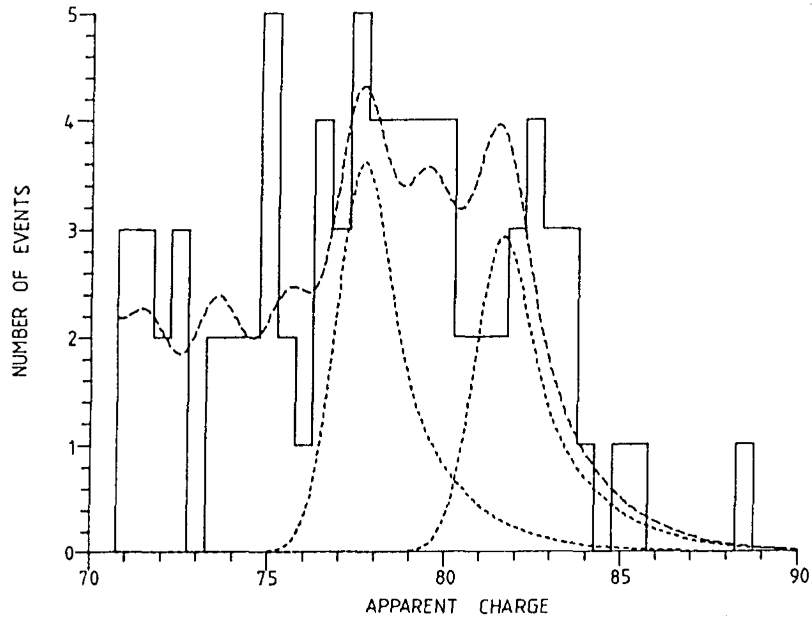

Fig. 2 Detail of the highest charges from Fig. 1. Dotted inserts show distributions for $_{78}Pt$ and $_{82}Pb$ content from Table 1.

Fig. 2 shows an expanded version of Fig. 1 for the $_{78}Pt$ - $_{82}Pb$ region alone. The inserted dotted lines show the predicted distribution in apparent charge of the $_{78}Pt$ and $_{82}Pb$ abundances obtained from the deconvolution. The tail of the $_{82}Pb$ distribution is seen to extend out to $Z_{app} \sim 88$ but only 0.1 event with $Z_{app} \gtrsim 90$ is predicted. Thus events with $84 \leq Z_{app} \leq 86$ are mainly the high energy $_{82}Pb$ nuclei which produce the exponential tail. Three events with $Z \geq 88$ were actually seen in this exposure, with Z_{app} 88.5, 93.5 and 97.0 following the non-Z^2 correction discussed in section 1.

3. Discussion. Data collection on Ariel VI allowed $_{26}Fe$ events to be recorded whenever the experiment was operational, with a continuously-measured efficiency. Consequently the normalisation of the data to abundances relative to $_{26}Fe = 10^6$ is straightforward. Column 3 of Table 1 shows normalised abundances, with a small correction added to allow for fragmentation in the material of the experiment, and these values are plotted as data points in Fig. 3 (together with the numbers from $34 \leq Z \leq 46$ for completeness). The numbers are compared with a recent propagation of Letaw et al. (7) which used solar system abundances modified by a first ionisation potential dependence, an exponential pathlength

distribution with characteristic length 6 gcm^{-2} of ISM and a propagation energy of 5 GeV/nucleon (histogram in Fig.3 and column 5 of Table 1). It is seen that the deconvolved Ariel VI abundances retain the over-abundance throughout the region $60 \leq Z \leq 80$ which has already been discussed (e.g. 7,8). The Ariel VI to Letaw et al. propagation ratio for $60 \leq Z \leq 82$ is 1.87 ± 0.14 based on 170 detected events. Letaw et al. attempted to go some way towards explaining this over-abundance by suggesting that propagation may take place mainly at a lower energy ($\sim$ 1 GeV/nucleon), where spallation into the $60 \leq Z \leq 74$ region is more favourable, but much of the discrepancy remains, the ratio being reduced only to 1.51 ± 0.12, suggesting an enhanced primary component in this region. The Letaw et al. propagations also produce consistently more $_{50}Sn$ than was seen in the Ariel VI data, and in that from HEAO3-C3 (9), which is shown for the charge region $50 \leq Z \leq 58$ in column 4 of Table 1 for comparison. Agreement between the two experiments is quite good in this region, but with a divergence of $\sim$ 3 s.d. at $_{52}Te$ where a separated peak is seen in the Ariel VI data.

For the highest charges, Binns et al. (10) quote a value for the abundance ratio $\dfrac{Z \geq 81}{74 \leq Z \leq 80}$ of 0.26 ± 0.08. Ignoring the three actinides our value for this ratio is 0.35 ± 0.12, higher, but not inconsistent with the HEAO value, and consistent with either the SS with no FIP fractionation or pure r-process with FIP fractionation values quoted in (10). Although the $_{82}Pb$ abundance seen in the Ariel VI data may not share the $60 \leq Z \leq 80$ over-abundance compared to propagated solar-system, it is not found to be depleted, being very close to the predicted abundance from the propagation.

Finally, three actinide candidates were seen in the Ariel VI exposure, compared to an expectation of 0.5 from the Brewster et al. propagation (11), a possible enhancement.

Fig. 3 Cosmic ray abundances normalised to $_{26}Fe = 10^6$. Data points are deconvolved abundances from Ariel VI corrected for fragmentation within the experiment. The histogram shows the Letaw et al. propagation of solar system material (7) referred to in the text.

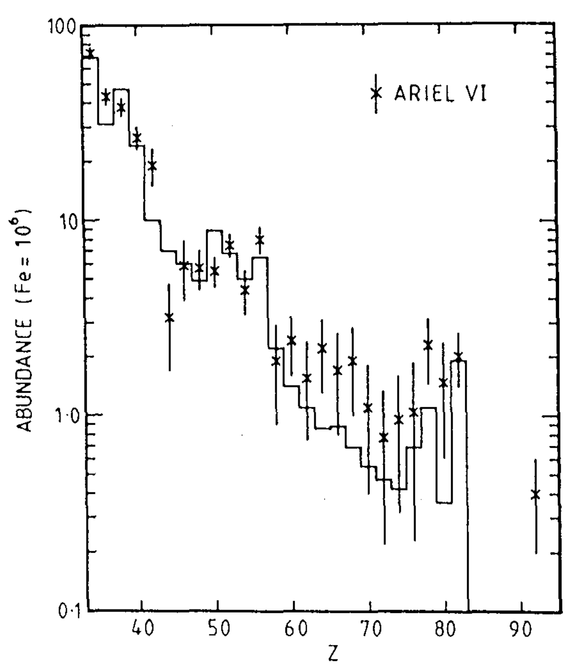

Table 1 Elemental Abundances for $Z \geq 48$

Z	Ariel VI Deconvolved Numbers	Ariel VI Corrected to outside expt.	HEAO3-C3	SS + FIPD Propagation, Letaw et al.
26	8.68×10^6	10^6	10^6	10^6
48	54 ± 12	5.7 ± 1.3		4.9
50	52 ± 9	5.5 ± 1.0	5.7 ± 1.3	8.9
52	68 ± 9	7.5 ± 1.0	3.4 ± 1.0	6.8
54	39 ± 10	4.4 ± 1.1	3.5 ± 0.9	5.0
56	69 ± 10	8.0 ± 1.2	6.2 ± 1.0	6.5
58	17 ± 9	1.9 ± 1.0	2.8 ± 0.9	2.2
60	22 ± 7	2.4 ± 0.8		1.4
62	14 ± 7	1.6 ± 0.8		1.1
64	20 ± 8	2.2 ± 0.9		0.86
66	15 ± 8	1.7 ± 0.9		0.88
68	17 ± 8	1.9 ± 0.9		0.69
70	10 ± 6	1.1 ± 0.7		0.55
72	7 ± 5	0.8 ± 0.6		0.47
74	9 ± 6	0.9 ± 0.6		0.42
76	9 ± 7	1.0 ± 0.8		0.69
78	19 ± 7	2.3 ± 0.8		1.1
80	12 ± 7	1.5 ± 0.9		0.36
82	16 ± 5	2.0 ± 0.6		1.9
84	0			
≥ 88	3	0.4 ± 0.2		

4. Acknowledgements. These are given in full in paper OG4.4-3.

5. References.

1. P.H. Fowler et al., 1979, Proc. 16th ICRC, Kyoto, 12, 338
2. J.A. Doggett et al., 1956, Phys. Rev. 103, 1597
3. S.P. Ahlen, 1978, Phys. Rev. (A), 17, 1236
4. J.H. Derrickson et al., 1981, Proc. 17th ICRC, Paris, 8, 88
5. C.J. Waddington et al., 1983, Phys. Rev. (A), 28, 464
6. T.L. Garrard et al., 1983, Proc. 18th ICRC, Bangalore, T2-10
7. J.R. Letaw et al., 1984, Ap. J. 279, 144
8. P.H. Fowler et al., 1981, Nature, 291, 45
9. E.C. Stone et al., 1983, Proc. 18th ICRC, Bangalore OG1-21
10. W.R. Binns et al., 1984, Adv. Space Res. 4, 25
11. N.R. Brewster et al., 1983, Ap. J. 264, 324